

Measurement and analysis of $^{155,157}\text{Gd}(n,\gamma)$ from thermal energy to 1 keV

C. Massimi^{1,2,*}, O. Aberle³, J. Andrzejewski⁴, L. Audouin⁵, M. Bacak^{6,3,7}, J. Balibrea⁸, M. Barbagallo⁹, F. Bečvář¹⁰, E. Berthoumieux⁷, J. Billowes¹¹, D. Bosnar¹², A. Brown¹³, M. Caamaño¹⁴, F. Calviño¹⁵, M. Calviani³, D. Cano-Ott⁸, R. Cardella³, A. Casanovas¹⁵, D. M. Castelluccio^{16,1}, F. Cerutti³, Y. H. Chen⁵, E. Chiaveri^{3,11,17}, G. Clai¹⁶, N. Colonna⁹, P. Console Camprini¹⁶, G. Cortés¹⁵, M. A. Cortés-Giraldo¹⁷, L. Cosentino¹⁸, L. A. Damone^{9,19}, M. Diakaki⁷, C. Domingo-Pardo²⁰, R. Dressler²¹, E. Dupont⁷, I. Durán¹⁴, B. Fernández-Domínguez¹⁴, A. Ferrari³, P. Ferreira²², P. Finocchiaro¹⁸, V. Furman²³, K. Göbel²⁴, A. R. García⁸, A. Gawlik⁴, S. Gilardoni³, T. Glodariu^{†25}, I. F. Gonçalves²², E. González-Romero⁸, E. Griesmayer⁶, C. Guerrero¹⁷, A. Guglielmelli¹⁶, F. Gunsing^{7,3}, H. Harada²⁶, S. Heinitz²¹, J. Heyse²⁷, D. G. Jenkins¹³, E. Jericha⁶, F. Käppeler²⁸, Y. Kadi³, A. Kalamara²⁹, P. Kavargin⁶, A. Kimura²⁶, N. Kivel²¹, I. Knapova¹⁰, M. Kokkoris²⁹, M. Krtička¹⁰, D. Kurtulgil²⁴, E. Leal-Cidoncha¹⁴, C. Lederer³⁰, H. Leeb⁶, J. Lerendegui-Marco¹⁷, S. J. Lonsdale³⁰, D. Macina³, A. Manna^{1,2}, J. Marganec⁴, T. Martínez⁸, A. Masi³, P. Mastinu³², M. Mastromarco⁹, E. A. Mauger²¹, A. Mazzone^{9,33}, E. Mendoza⁸, A. Mengoni¹⁶, P. M. Milazzo³⁴, F. Mingrone³, R. Mucciola^{1,2}, A. Musumarra^{18,35}, A. Negret²⁴, R. Nolte³¹, A. Oprea²⁴, N. Patronis³⁶, A. Pavlik³⁷, J. Perkowski⁴, I. Porras³⁸, J. Praena³⁸, J. M. Quesada¹⁷, D. Radeck³¹, T. Rauscher^{39,40}, R. Reifarth²⁴, F. Rocchi¹⁶, C. Rubbia³, J. A. Ryan¹¹, M. Sabaté-Gilarte^{3,17}, A. Saxena⁴¹, P. Schillebeeckx²⁷, D. Schumann²¹, P. Sedyshev²³, A. G. Smith¹¹, N. V. Sosnin¹¹, A. Stamatopoulos²⁹, G. Tagliente⁹, J. L. Tain²⁰, A. Tarifeño-Saldivia¹⁵, L. Tassan-Got⁵, S. Valenta¹⁰, G. Vannini^{1,2}, V. Variale⁹, P. Vaz²², A. Ventura¹, V. Vlachoudis³, R. Vlastou²⁹, A. Wallner⁴², S. Warren¹¹, C. Weiss⁶, P. J. Woods³⁰, T. Wright¹¹, and P. Žugec^{12,3}
the n_TOF Collaboration

¹Istituto Nazionale di Fisica Nucleare, Sezione di Bologna, Italy

²Dipartimento di Fisica e Astronomia, Università di Bologna, Italy

³European Organization for Nuclear Research (CERN), Switzerland

⁴University of Lodz, Poland

⁵Institut de Physique Nucléaire, CNRS-IN2P3, Univ. Paris-Sud, Université Paris-Saclay, F-91406 Orsay Cedex, France

⁶Technische Universität Wien, Austria

⁷CEA Irfu, Université Paris-Saclay, F-91191 Gif-sur-Yvette, France

⁸Centro de Investigaciones Energéticas Medioambientales y Tecnológicas (CIEMAT), Spain

⁹Istituto Nazionale di Fisica Nucleare, Sezione di Bari, Italy

¹⁰Charles University, Prague, Czech Republic

¹¹University of Manchester, United Kingdom

¹²Department of Physics, Faculty of Science, University of Zagreb, Zagreb, Croatia

¹³University of York, United Kingdom

¹⁴University of Santiago de Compostela, Spain

¹⁵Universitat Politècnica de Catalunya, Spain

¹⁶Agenzia nazionale per le nuove tecnologie (ENEA), Bologna, Italy

¹⁷Universidad de Sevilla, Spain

¹⁸INFN Laboratori Nazionali del Sud, Catania, Italy

¹⁹Dipartimento di Fisica, Università degli Studi di Bari, Italy

²⁰Instituto de Física Corpuscular, CSIC - Universidad de Valencia, Spain

²¹Paul Scherrer Institut (PSI), Villingen, Switzerland

²²Instituto Superior Técnico, Lisbon, Portugal

²³Joint Institute for Nuclear Research (JINR), Dubna, Russia

²⁴Goethe University Frankfurt, Germany

²⁵Horia Hulubei National Institute of Physics and Nuclear Engineering, Romania

²⁶Japan Atomic Energy Agency (JAEA), Tokai-mura, Japan

²⁷European Commission, Joint Research Centre, Geel, Retieseweg 111, B-2440 Geel, Belgium

²⁸Karlsruhe Institute of Technology, Campus North, IKP, 76021 Karlsruhe, Germany

²⁹National Technical University of Athens, Greece

³⁰School of Physics and Astronomy, University of Edinburgh, United Kingdom

³¹Physikalisch-Technische Bundesanstalt (PTB), Bundesallee 100, 38116 Braunschweig, Germany

³²Istituto Nazionale di Fisica Nucleare, Sezione di Legnaro, Italy

³³Consiglio Nazionale delle Ricerche, Bari, Italy

³⁴Istituto Nazionale di Fisica Nucleare, Sezione di Trieste, Italy

³⁵Dipartimento di Fisica e Astronomia, Università di Catania, Italy

³⁶University of Ioannina, Greece

³⁷University of Vienna, Faculty of Physics, Vienna, Austria

³⁸University of Granada, Spain

³⁹Department of Physics, University of Basel, Switzerland

⁴⁰Centre for Astrophysics Research, University of Hertfordshire, United Kingdom

⁴¹Bhabha Atomic Research Centre (BARC), India

⁴²Australian National University, Canberra, Australia

Abstract. We have measured the capture cross section of the ^{155}Gd and ^{157}Gd isotopes between 0.025 eV and 1 keV. The capture events were recorded by an array of 4 C_6D_6 detectors, and the capture yield was deduced exploiting the total energy detection system in combination with the Pulse Height Weighting Techniques. Because of the large cross section around thermal neutron energy, 4 metallic samples of different thickness were used to prevent problems related to self-shielding. The samples were isotopically enriched, with a cross contamination of the other isotope of less than 1.14%. The capture yield was analyzed with an R-Matrix code to describe the cross section in terms of resonance parameters. Near thermal energies, the results are significantly different from evaluations and from previous time-of-flight experiments. The data from the present measurement at n_TOF are publicly available in the experimental nuclear reaction database EXFOR.

1 Introduction

The large capture cross section of gadolinium has considerable influence on applications in nuclear technologies [1, 2] and has significant impact in neutrino physics, hadron therapy and nuclear astrophysics.

The values of the ^{155}Gd and ^{157}Gd thermal cross sections retrieved from the experimental nuclear reaction database EXFOR [3] reported in refs. [4–9] are reported together with ENDF/B-VIII.0 [10], CENDL-3.1 [11], JEFF-3.3 [12] and JENDL-4.0 [13] nuclear data libraries and the compilation by Mughabghab [14] in Table 1. Other measurements are not listed because they are not direct measurements of the cross section, whose value cannot be reconstructed from the reported experimental observables. The tabulated cross sections show that large deviations, as high as 11%, with respect to the last evaluation, namely ENDF/B-VIII.0, are present in literature.

The request for high accuracy data for the gadolinium isotopes with the largest capture cross section [15] motivated a new measurement of these two isotopes at the neutron time-of-flight facility n_TOF [16] at CERN. The details of the experiment, data analysis and results of the n_TOF experiment have been published in ref. [9]. In this conference proceedings we prove the quality of the R-matrix analysis of the experimental data and provide required details to use the n_TOF data available on EXFOR for future evaluations.

2 Measurement

The capture measurement was performed at the n_TOF facility at CERN in 2016 [9]. The longest flight path, at 184 m from the neutron source, was used to take advantage of the better energy resolution. The experimental setup consisted of an array of 4 C_6D_6 for the measurement of the capture events and of a ^6Li -based detector for the determination of the neutron flux impinging on the gadolinium samples.

For each isotope, two samples of different thickness were used. The areal density of the ^{155}Gd samples was

$(1.244 \pm 0.004) \times 10^{-4}$ and $(1.236 \pm 0.012) \times 10^{-5}$ atoms/b, whereas for the ^{157}Gd samples it was $(2.339 \pm 0.006) \times 10^{-4}$ and $(5.74 \pm 0.12) \times 10^{-6}$ atoms/b. The samples were in the form of self-supporting metal discs, highly enriched in the isotope of interest. In addition to the 4 gadolinium samples, ^{197}Au and lead samples were used for normalisation and for the determination of the background. All the samples were circular in shape with a radius of 1 cm. Particular care was devoted to develop a system able to guarantee an excellent repeatability of sample position and its alignment with respect to the neutron beam. An empty-sample was prepared, as a replica of the Gd samples excluding the metal disc, and it was measured during the campaign to estimate the sample-independent background induced by the neutron beam.

The flux was evaluated with respect to the $^6\text{Li}(n,t)\alpha$ reaction standard [17]. The flux detector [18] consisted of a $600 \mu\text{g}/\text{cm}^2$ LiF foil placed in the beam, viewed off-beam by 4 silicon detectors ($5 \text{ cm} \times 5 \text{ cm} \times 300 \mu\text{m}$). In the data analysis a correction to take into account the absorption of neutrons passing through the LiF foil was applied.

3 Analysis

The total energy principle was applied by combining the detection system based on C_6D_6 liquid scintillation detectors with the Pulse Height Weighting Technique (PHWT) [19], which assures the proportionality of the detection efficiency and the corresponding γ -ray energy. As a consequence, this technique makes the efficiency to detect a capture event proportional to the Q-value of the nuclear reaction. A problem arises when the sample contains more than one isotope, since the Q-value is different for each isotope. Therefore, to apply this well-established measurement principle, an approximation was required. In the simultaneous resonance shape analysis of the capture yields with the SAMMY [20] R-Matrix code, the abundance of the contaminant isotopes was scaled accordingly to the Q-value (*i.e.* the abundance of a contaminant is divided by its Q-value of the neutron capture reaction and is multiplied by that of the isotope of interest). This modification, which introduced a negligible bias on the multi-

*e-mail: massimi@bo.infn.it

Table 1. ^{155}Gd and ^{157}Gd thermal cross sections (in kb) as reported in literature, compilation [14] and evaluations. The results from the present measurement are reported for comparison.

Reference	Year	Type	$n + ^{155}\text{Gd}$	deviation to ENDF/B-VIII.0	$n + ^{157}\text{Gd}$	deviation to ENDF/B-VIII.0
Møller [4]	1960	TOF	58.9(5) ^a	-3.3%	254(2) ^a	0.27%
Ohno [5]	1968	TOF	61.9(6) ^a	1.7%	248(4) ^a	-2.10%
Leinweber [6]	2006	TOF	60.2	-1.1%	226	-11%
Noguere [7]	2011	Pile oscillation	61.9(15)	1.7%		
Choi [8]	2014	Spectra averaged	56.7(21)	-6.9%	239(6)	-5.7%
Mughabghab [14]	2009	Compilation	60.9(5)	0.02%	254.0(8)	0.27%
CENDL-3.1 [11]	2009	Evaluation	60.888	-	254.01	0.27%
JENDL-4.0 [13]	2011	Evaluation	60.735	-0.25%	253.25	-0.03%
JEFF-3.3 [12]	2017	Evaluation	60.89	-	254.5	0.47%
ENDF/B-VIII.0 [10]	2018	Evaluation	60.89	-	253.32	-
Mastromarco [9]	2019	TOF	62.2(22)	2.2%	239.8(84)	-5.3%

^a Total cross section.

ple scattering correction, made the calculated capture yield consistent with the experimental capture yield.

In Table 2 the abundances of the gadolinium isotopes in the ^{155}Gd and ^{157}Gd samples are listed together with the corresponding quantity used in the resonance shape analysis. It is worth noticing that the cross contamination of the ^{155}Gd isotope in the enriched ^{157}Gd samples and the one of the ^{157}Gd isotope in the enriched ^{155}Gd sample is less than 1.14%.

4 Discussion on uncertainties

The systematic uncertainties of the experimental capture yield come from: (i) normalisation, (ii) PHWT, (iii) background subtraction, (iv) sample characterisation, (v) neutron flux shape, and, in the energy region below 1 eV, (vi) the uncertainty related to the beam interception factor. More details on the assessment of the different components can be found in ref. [9]. We remind the reader that the individual contributions to the total uncertainty were very similar. It can be argued that at thermal energy the uncertainty component (v) due to neutron flux shape already incorporates the uncertainty component (vi) related to the beam interception factor and therefore the total uncertainty is slightly lower than reported in ref. [9] being reduced to 3% and 3.4%, respectively for the thermal cross section of $^{155}\text{Gd}(n,\gamma)$ and $^{157}\text{Gd}(n,\gamma)$.

To further decrease the total uncertainty, the samples are now being analyzed in order to reduce the uncertainty related to the sample mass and its distribution. In particular a transmission experiment on the same samples is ongoing at the GELINA facility at JRC Geel (Belgium) and a proton elastic backscattering experiment is also foreseen for the near future.

5 Results

From a simultaneous resonance shape analysis of the capture yields, using the R-Matrix code SAMMY, the cross sections were parametrized in terms of resonance parameters in the energy region from thermal to 1 keV neutron

energy. An example of the good quality of the fitting procedure is shown in Fig.1 for both gadolinium isotopes.

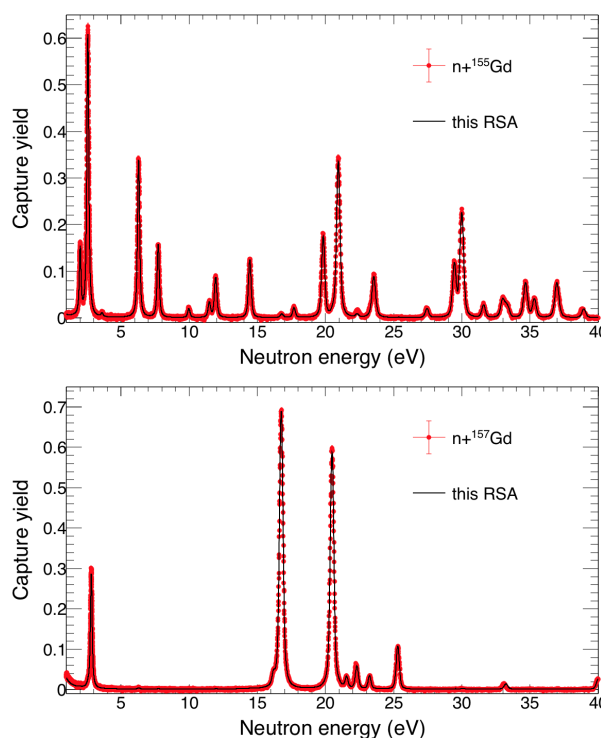


Figure 1. (Color online) $^{155,157}\text{Gd}(n,\gamma)$ capture yields from the present experiment and results of the resonance shape analysis (RSA) in the neutron energy region from 1 to 40 eV.

The results of the resonance shape analysis were used to reconstruct the cross section and in particular to evaluate the thermal cross section and the Westcott factor. These values are reported in Table 3 for ^{155}Gd and ^{157}Gd .

The updated resonance parameters were also used to determine the basic statistical properties of the neutron resonances in $n+^{155}\text{Gd}$ and $n+^{157}\text{Gd}$ systems. Neutron strength function and level spacing resulted fully consistent with values in literature, whereas the estimated $\bar{\Gamma}_\gamma =$

Table 2. Isotopic composition of the gadolinium isotopes and corresponding scaled quantity used in the resonance shape analysis (the Q-value of the (n, γ) reaction adopted for the calculation of the abundance used in SAMMY is reported).

Isotope (natural abund.)	Q-value (MeV)	¹⁵⁵ Gd samples		¹⁵⁷ Gd samples	
		Declared	Scaled	Declared	Scaled
¹⁵² Gd (0.2%)	6.246	0.03%	0.03%	< 0.01%	< 0.008%
¹⁵⁴ Gd (2.18%)	6.435	0.63 ± 0.02%	0.47 ± 0.015%	0.04 ± 0.01%	0.032 ± 0.008%
¹⁵⁵ Gd (14.80%)	8.536	91.74 ± 0.18%	91.74 ± 0.18%	0.29 ± 0.01%	0.31 ± 0.01%
¹⁵⁶ Gd (20.47%)	6.36	5.12 ± 0.18%	3.81 ± 0.13%	1.68 ± 0.01%	1.346 ± 0.008%
¹⁵⁷ Gd (15.65%)	7.937	1.14%	1.06%	82.32 ± 0.01%	88.32 ± 0.01%
¹⁵⁸ Gd (24.84%)	5.943	0.94 ± 0.09%	0.65 ± 0.06%	9.10 ± 0.01%	6.814 ± 0.007%
¹⁶⁰ Gd (21.86%)	5.635	0.40 ± 0.07%	0.26 ± 0.05%	0.57 ± 0.01%	0.405 ± 0.007%

Table 3. Capture cross section and Westcott factor deduced from the n_TOF data.

Isotope	Thermal cross section	Westcott factor
¹⁵⁵ Gd	62.2(20) kb	0.89(4)
¹⁵⁷ Gd	239.8(81) kb	0.86(4)

106.8(14) and 101.1(20) meV, respectively for ¹⁵⁵Gd and ¹⁵⁷Gd, are slightly different from literature.

6 Conclusion

The ¹⁵⁵Gd(n, γ) and ¹⁵⁷Gd(n, γ) cross section measurements were performed at the n_TOF facility. They provided thermal cross sections at $E_n = 0.0253$ eV of 62.2(20) kb and 239.8(81) kb, respectively. The percentage deviation to ENDF/B-VIII.0 is sizable, in particular for ¹⁵⁷Gd, while fair agreement was found for ¹⁵⁵Gd. In terms of standard deviations, the present ¹⁵⁷Gd(n, γ) cross section is approximately two sigma away from evaluations. To make this result more conclusive, a series of complementary measurements and studies are ongoing to reduce the uncertainty related to the present R-matrix parametrization.

The results of the capture yields obtained at n_TOF are available in the EXFOR database, and they can be used for future evaluations.

Acknowledgments

The isotopes used in this research were supplied by the United States Department of Energy Office of Science by the Isotope Program in the Office of Nuclear Physics.

This research was partially funded by the European Atomic Energy Community (Euratom) Seventh Framework Programme FP7/2007-2011 under the Project CHANDA (Grant No. 605203).

We acknowledge support from FPA2014-52823-C2-1-P (MINECO) and MSMT Czech Republic.

We thank Naohiko Otsuka for his valuable effort to prepare the EXFOR entry #23400.

References

[1] F. Rocchi, A. Guglielmelli, D. M. Castelluccio and C. Massimi, *Eur. Phys. J. Nuclear Sci. Technol.* **3**, 21 (2017)

[2] F. Rocchi, A. Guglielmelli, P. Console Camprini, C. Massimi and Luiz Leal, *Annals of Nuclear Energy* **132**, 537 (2019)

[3] N. Otuka, *et. al.*, *Nucl. Data Sheets* **120**, 272 (2014)

[4] H. Bjerrum Møller, F. J. Shore, and V. L. Sailor, *Nucl. Sci. Eng.* **8**, 183 (1960)

[5] Y. Ohno, *et. al.*, Japanese report to EANDC, Number 10, p. 1 (1968)

[6] G. Leinweber, *et. al.*, *Nucl. Sci. Eng.* **154**, 261 (2006)

[7] G. Noguere, P. Archier, A. Gruel, P. Leconte and D. Bernard, *Nucl. Instrum. & Methods A* **629**, 288 (2011)

[8] H.D.Choi, *et. al.*, *Nucl. Science & Eng.* **177**, 219 (2014)

[9] M. Mastromarco, *et al.*, *Eur. Phys. J. A* **55**, 9 (2019)

[10] D. A. Brown, *et. al.*, *Nucl. Data Sheets* **148**, 1 (2018)

[11] Z. G. Ge, Y. X. Zhuang, T. J. Liu, J. S. Zhang, H. C. Wu, Z. X. Zhao, H. H. Xia, *Journal of the Korean Physical Society* **59(2)**, 1052 (2011)

[12] A. Plompen, *et. al.*, The Joint Evaluated Fission and Fusion Nuclear Data Library, JEFF-3.3, *Eur. Phys. J. A*, accepted for publication

[13] K. Shibata, *et. al.*, *J. Nucl. Sci. Technol.* **48**, 1 (2011)

[14] S. F. Mughabghab, *Atlas of Neutron Resonances* (Elsevier, Amsterdam, 2006)

[15] A. Plompen, *et. al.*, The NEA High Priority Nuclear Data Request List for future needs, *Int. Conf. on Nuclear Data for Science and Technology*, (2007) 765

[16] C. Guerrero, *et al.*, *Eur. Phys. J. A* **49**, 27 (2013)

[17] A. D. Carlson, *et al.*, *Nucl. Data Sheets* **110**, 3215 (2009)

[18] S. Marrone, *et al.*, *Nucl. Instrum. & Methods A* **517**, 389 (2004)

[19] P. Schillebeeckx, *et al.*, *Nucl. Data Sheets* **113**, 3054 (2012)

[20] N. M. Larson, "Updated Users Guide for SAMMY: Multilevel R-matrix Fits to Neutron Data Using Bayes Equations, SAMMY", Computer Code, Report No. ORNL/TM-9179/R7, Oak Ridge National Laboratory, 2008